

Phase transformation of mixed-phase clouds

By ALEXEI KOROLEV* and GEORGE ISAAC
Meteorological Service of Canada, Canada

(Received 13 December 2001; revised 7 May 2002)

SUMMARY

The glaciation time of a mixed-phase cloud due to the Wegener–Bergeron–Findeisen mechanism is calculated using an adiabatic one-dimensional numerical model for the cases of zero, ascending, descending and oscillating vertical velocities. The characteristic values of the glaciation time are obtained for different concentrations of ice particles and liquid-water content. Steady state is not possible for the ice-water content/total water content ratio in a uniformly vertically moving mixed-phase parcel. The vertical oscillation of a cloud parcel may result in a periodic evaporation and activation of liquid droplets in the presence of ice particles during infinite time. After a certain time, the average ice-water content and liquid-water content reach a steady state. This phenomenon may explain the existence of long-lived mixed-phase stratiform layers. The obtained results are important for understanding the mechanisms of formation and life cycle of mixed-phase clouds.

KEYWORDS: Glaciation time

1. INTRODUCTION

The saturation vapour pressure over liquid water is higher than that over ice at low temperatures. Therefore, the growth rate of ice particles and liquid droplets under the same conditions will be different. As a result an *adiabatic* colloidal three-phase component system consisting of water vapour, ice particles and liquid droplets becomes condensationally unstable and may exist during a limited period of time. At the final stage, all the liquid droplets will evaporate and the system will consist only of ice particles and water vapour. The glaciation process due to ice growth by deposition at the expense of co-existing liquid droplets is known as the Wegener–Bergeron–Findeisen (hereafter WBF) mechanism (Wegener 1911; Bergeron 1935; Findeisen 1938).

Interactions between ice particles and liquid droplets in mixed-phase clouds have been considered in a large variety of numerical models (e.g. Scott and Hobbs 1977; Hall 1980; Cotton and Anthes 1989; Houze 1992; Reisin *et al.* 1996; Lohmann and Roeckner 1996; Tremblay *et al.* 1996; Harrington *et al.* 1999; Jiang *et al.* 2000; Rotstain *et al.* 2000; Zawadzki *et al.* 2000 to name a few of them). Most numerical models considering mixed-phase clouds take into account ice growth due to the WBF mechanism. However, the role of the WBF mechanism is in many ways masked by the effects of ice multiplication, riming, aggregation, and terminal fall velocity.

The purpose of this paper is to study the glaciation time of mixed-phase clouds under different conditions solely due to the WBF mechanism.

The glaciation of mixed-phase clouds has been studied in a number of works. Juisto (1971) modelled glaciation of uniformly ascending cloud parcels. Mazin (1983) theoretically studied the glaciation time for mixed clouds for a zero updraught velocity. Rauber and Tokay (1991) attempted to explain observations of long-lived narrow layers of supercooled water at cloud tops existing down to -30°C . Using a one-dimensional numerical model, they showed that the imbalance between the condensate supply rate and the bulk ice crystal mass growth rate at a wide range of updraught speeds is sufficient to produce a liquid layer near the cloud top. Tremblay *et al.* (1996) showed that a steady-state condition for the fraction of ice is possible for mixed cloud during ascent. As a result, a complete glaciation due to the WBF mechanism would never

* Corresponding author: 28 Don Head Village Blvd., Richmond Hill, Ontario L4C 7M6, Canada.
e-mail: Alexei.Korolev@rogers.com

occur in a uniformly ascending parcel. Harrington *et al.* (1999) using a cloud-resolving model demonstrated that cloud layers may either collapse through rapid glaciation and precipitation from the cloud, or maintain a quasi-steady state. Removal of ice freezing nuclei (IFN) from the cloud layer by falling out ice particles appears to be of prime importance to the stability of the cloud layer. Pinto (1998) came to similar conclusions regarding the importance of IFN sources and removal using data from the Beaufort and Arctic Storms Experiment. Harrington *et al.* (1999) also suggested the importance of ice concentration in the evolution of mixed-phase clouds. Rotstajn *et al.* (2000) studied the formation of the distribution of liquid fraction in mixed clouds for zero updraught velocity. It was shown that the modelled distribution of the liquid fraction is wider as compared with that measured by Bower *et al.* (1996) when a supersaturation-dependent parametrization of ice crystal concentration (Meyers *et al.* 1992) was used. Fletcher's (1962) parametrization resulted in a too high a liquid fraction. The liquid fraction was found to be sensitive to ice particle habits and the spatial inhomogeneity of ice. Zawadzki *et al.* (2000) modelled formations of ice and liquid water in uniformly ascending cloud parcels.

For this work, the glaciation time was simulated for the cases of zero, ascending, descending, and oscillating vertical velocity for an adiabatic mixed-phase cloud parcel with the help of a simple one-dimensional model. The obtained results are important for better understanding the mechanisms of formation and life cycle of mixed-phase clouds.

2. GLACIATION TIME OF MIXED-PHASE CLOUDS

(a) Case $U_z = 0$

The glaciation time can be estimated analytically for the case of zero vertical velocity, $U_z = 0$, when only deposition–sublimation for ice particles and condensation–evaporation for liquid droplets are taken into account. Consider an adiabatic cloud volume consisting of evenly mixed liquid droplets and ice particles. For simplicity assume that the ice particles are monodisperse spheres. During the ice growth the droplets will evaporate, maintaining the water vapour pressure nearly constant and close to saturation over water. The mass growth of a spherical ice particle can be written as (e.g. Fukuta and Walter 1970)

$$\frac{dm_i}{dt} = 4\pi A_i c r_i S_i. \quad (1)$$

Here

$$S_i = \frac{E_{sw}(T) - E_{si}(T)}{E_{si}(T)}$$

is the supersaturation over an ice surface; $E_{sw}(T)$, $E_{si}(T)$ are the saturation vapour pressure at temperature T over flat water and ice surfaces, respectively; r_i is the radius of ice particles; c is a constant ‘capacitance’ representing the ice crystal habit ($0 < c \leq 1$; for ice spheres $c = 1$);

$$A_i = \left(\frac{L_i^2}{k R_v T^2} + \frac{R_v T}{E_i(T) D} \right)^{-1},$$

where L_i is the latent heat for ice; E_i is the vapour pressure over ice, R_v is the specific gas constant of water vapour, $D(T, P)$ is the coefficient of water vapour diffusion in the air, P is pressure and $k(T)$ is the coefficient of air heat conductivity.

With these assumptions, the ice particles are growing at the expense of liquid droplets only. Therefore at the moment of glaciation (τ_{gl}), the mass of all ice particles will be

$$W_{\text{IWC}}(\tau_{\text{gl}}) = W_{\text{IWC}}(t_0) + W_{\text{LWC}}(t_0). \quad (2)$$

Here $W_{\text{LWC}}(t_0)$ and $W_{\text{IWC}}(t_0)$ are initial masses of liquid and ice in the cloud volume. Hence, assuming that the ice particles are monodisperse, the individual ice particle mass at the initial moment of time $t_0 = 0$ is

$$m_i(t_0) = \frac{W_{\text{IWC}}(t_0)}{N_i}. \quad (3)$$

Assuming that the number concentration of the ice particles, N_i , stays constant, the mass of a single ice particle at the moment of glaciation will be

$$m_i(\tau_{\text{gl}}) = \frac{W_{\text{IWC}}(\tau_{\text{gl}})}{N_i} = \frac{W_{\text{IWC}}(t_0) + W_{\text{LWC}}(t_0)}{N_i}. \quad (4)$$

Integrating Eq. (1) from $m_i(t_0)$ to $m_i(\tau_{\text{gl}})$ and substituting Eqs. (3) and (4) yields the glaciation time

$$\tau_{\text{gl}} = \frac{1}{4\pi c A_i S_i} \left(\frac{9\pi \rho_i}{2} \right)^{1/3} \left\{ \left(\frac{W_{\text{LWC}0} + W_{\text{IWC}0}}{N_i} \right)^{2/3} - \left(\frac{W_{\text{IWC}0}}{N_i} \right)^{2/3} \right\}, \quad (5)$$

where ρ_i is the density of ice.

If $W_{\text{LWC}}(t_0) \gg W_{\text{IWC}}(t_0)$ then Eq. (5) will be simplified (Mazin 1983; Mazin *et al.* 2000)

$$\tau_{\text{gl}} = \frac{1}{4\pi c A_i S_i} \left(\frac{9\pi \rho_i}{2} \right)^{1/3} \left(\frac{W_{\text{LWC}0}}{N_i} \right)^{2/3}. \quad (6)$$

Equation (5) indicates that the time of glaciation is insensitive to a first approximation to the size spectra of liquid droplets, and depends only on ice particle number concentration and initial liquid-water content (LWC) and ice-water content (IWC). Figure 1 shows the dependence of τ_{gl} versus T for different N_i calculated from a numerical model (see appendix), and that derived from Eq. (5). The calculations were done for $W_{\text{LWC}0} = 0.1 \text{ g kg}^{-1}$ and altitude $H = 3000 \text{ m}$ ($P \cong 644 \text{ mb}$ to 685 mb depending on T). As seen from Fig. 1, τ_{gl} has a minimum around -12°C , where the difference between the saturation vapour pressure over water and ice has a maximum. The glaciation time increases towards 0°C and cold temperatures where the difference $E_{\text{sw}}(T) - E_{\text{si}}(T)$, and therefore S_i , approaches zero.

The agreement between Eq. (5) and the numerical model is surprisingly good for ice concentrations less than 1000 l^{-1} . The error between the numerical model and Eq. (5) increases with an increase of N_i (Fig. 1). For example, for $N_i = 10^4 \text{ l}^{-1}$ and $N_i = 10^3 \text{ l}^{-1}$ the relative error at $T = -15^\circ \text{C}$ reaches about 40% and 5%, respectively. For ice concentrations less than $N_i = 10^2 \text{ l}^{-1}$, the maximum relative error between the model and Eq. (5) does not exceed 1%. Therefore Eqs. (5) and (6) can be applied for a practical estimation of τ_{gl} . The agreement between Eq. (5) and the numerical model indicates that in mixed-phase clouds with no updraught the vapour pressure is close to saturation over liquid water before evaporation of liquid droplets is completed, and the rate of decrease of LWC is equal to the rate of growth of IWC.

Besides temperature, the glaciation time is also a function of pressure. Figure 2 shows τ_{gl} versus pressure converted into altitude. The glaciation time decreases with a

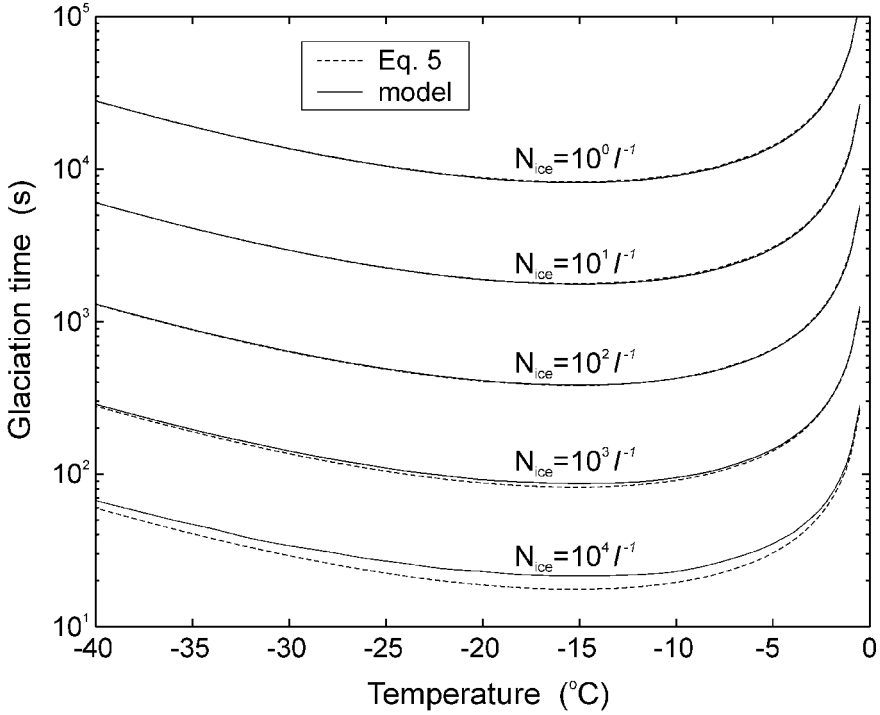


Figure 1. Time of glaciation, calculated using a numerical model and also derived using Eq. (5), versus temperature for zero vertical velocity at 3000 m with a liquid-water content of 0.1 g kg^{-1} for various number concentrations of ice particles.

decrease of pressure (an increase of height). At $T = -40 \text{ }^\circ\text{C}$ τ_{gl} changes by about one order of magnitude from 0 to 10 km in altitude. The grey colour in Fig. 2 indicates the conditions where T and P change in accordance with the Standard Atmosphere for winter (stars) and summer (circles) conditions (McClatchey *et al.* 1972). As seen from Fig. 2, τ_{gl} may change by a factor of two for the same W_{LWC} and N_i , depending on the altitude.

The glaciation time in Fig. 2 was calculated for $W_{\text{LWC}}(t_0) = 0.1 \text{ g kg}^{-1}$ and $N_i = 100 \text{ l}^{-1}$. To find τ_{gl} for different $W_{\text{LWC}}(t_0)$ and N_i one should simply scale the results in Figs. 1 and 2 by the factor $10^2 (W_{\text{LWC}0}/N_i)^{2/3}$, where $W_{\text{LWC}0}$ is in g kg^{-1} and N_i is in l^{-1} .

If the ice particles are not spherical, i.e. $c < 1$, then the glaciation time should be scaled up by the factor of c^{-1} (Eq. (5)).

(b) Case $U_z > 0$

Adiabatic cooling in an ascending parcel serves as a source of supersaturation, thus affecting the rate of growth of liquid and ice particles and resulting in changes in the glaciation time. Depending on U_z , LWC may both monotonically decrease all the time or first increase during some period of time and then decrease. This behaviour is demonstrated in Fig. 3 showing the results of the numerical model (see appendix) of LWC, IWC, and total water content (TWC) (Fig. 3(a)), droplet and ice particle sizes (Fig. 3(b)) and supersaturation (Fig. 3(c)) versus altitude for two different velocities U_z . The model was run with $N_i = 10^3 \text{ l}^{-1}$, $W_{\text{LWC}0} = 0.1 \text{ g kg}^{-1}$, $T_0 = -10 \text{ }^\circ\text{C}$, $H_0 =$

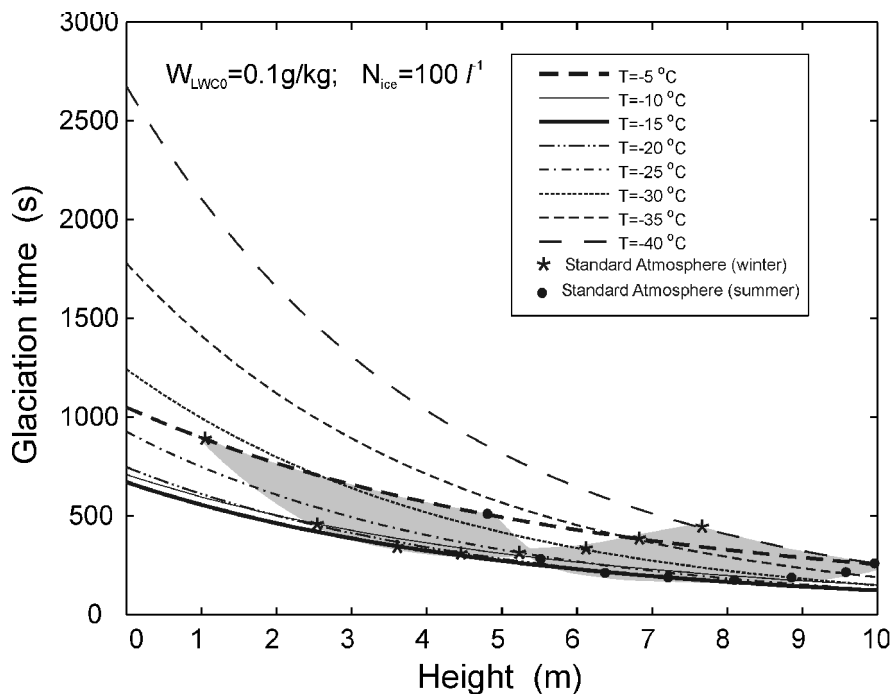


Figure 2. Time of glaciation versus altitude (converted from pressure) for different temperatures and for zero vertical velocity. The grey area indicates conditions for the summer and winter Standard Atmosphere. See text for further explanation.

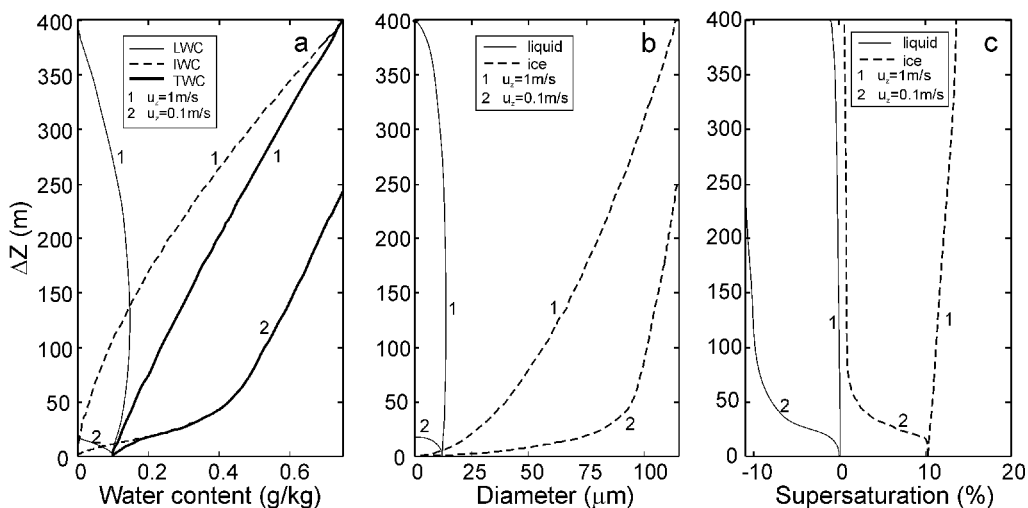


Figure 3. Modelling of phase transformation in a uniformly ascending parcel for two different vertical velocities (1) = 1 m s^{-1} and (2) = 0.1 m s^{-1} . Variation of (a) ice-water content (IWC), liquid-water content (LWC) and total water content (TWC), (b) liquid droplets and ice particle diameters; and (c) supersaturation over ice and liquid water. $N_i = 1000 \text{ l}^{-1}$, $T_0 = -10^\circ\text{C}$ and $H_0 = 1000 \text{ m}$ (see text).

1000 m. As seen from Fig. 3(a) at $U_z = 0.1 \text{ m s}^{-1}$, LWC decreases all the time, whereas at $U_z = 1 \text{ m s}^{-1}$ LWC first increases and then decreases.

During ascent the temperature and pressure inside the cloud parcel are continuously changing. This adds complexity to the phase transformation in a vertically moving parcel. Figures 4(a), (b) and (c) show τ_{gl} versus U_z for (a) different N_i , (b) initial $W_{\text{LWC}0}$, and (c) T_0 . Figures 4(b) and (c) show that, depending on $W_{\text{LWC}0}$ and T_0 , τ_{gl} may both increase and decrease with an increase of U_z . Numerical modelling shows that for an ice concentration $N_i = 10^3 \text{ l}^{-1}$ and water content $W_{\text{LWC}0} > 1.6 \text{ g kg}^{-1}$, τ_{gl} decreases first and then increases with an increase of U_z (Fig. 4(b)). For larger N_i and lower $W_{\text{LWC}0}$ τ_{gl} would monotonically increase with an increase of U_z . For $W_{\text{LWC}0} = 0.1 \text{ g kg}^{-1}$, $T_0 = -5^\circ \text{C}$ and $N_i = 10^3 \text{ l}^{-1}$, τ_{gl} would increase about five times when U_z increases from 0 to 4 m s^{-1} (Figs. 4(a) and (c)).

Figures 4(d), (e) and (f) show sizes of ice particles D_{gl} at the moment of glaciation. The size D_{gl} monotonically increases with an increase of the updraught velocity U_z . As seen from Fig. 4(d), at low ice concentrations, $N_i < 10^2 \text{ l}^{-1}$, D_{gl} , and therefore its terminal velocity, may become high enough that it would fall out of the cloud making the modelling results inaccurate. This modelling problem will be discussed in more detail in section 3(a).

If the vertical velocity is high enough, then the liquid droplets may not evaporate by the time the parcel reaches the temperature of homogeneous freezing $T = -40^\circ \text{C}$ (Pruppacher and Klett 1997). At this point, all droplets in the parcel are assumed to turn into ice instantly. In Fig. 4, the glaciation time for the cases when the parcels reach the temperature below that of spontaneous glaciation is shown by dashed lines.

It is worth noting that, for $U_z > 4 \text{ m s}^{-1}$ with $N_i < 10^3 \text{ l}^{-1}$ for any $W_{\text{LWC}0}$, the concentration of ice particles is not enough to glaciare the cloud though the WBF mechanism, and glaciation occurs at the cloud tops through homogeneous freezing when the parcel reaches $T = -40^\circ \text{C}$. This conclusion is important for understanding the mechanisms of phase transformation in convective clouds.

(c) Case $U_z < 0$

In stratiform layers, the ascending and descending motions have approximately equal probability. Therefore, glaciation in descending parcels may play as important a role in the phase composition formation of clouds as in ascending ones.

First, consider a descending cloud parcel consisting only of liquid droplets without ice particles. Assume that all processes inside the parcel are adiabatic. During descent the temperature inside the parcel will increase due to adiabatic heating. As a result, the supersaturation becomes negative and the droplets start evaporating, reducing LWC. For the assumption that condensation inertia effects can be neglected, the LWC value will decrease following its adiabatic value. At some level the LWC will become zero. The vertical distance undergone by the parcel before complete evaporation of LWC can be found as (Korolev and Mazin 1993)

$$\Delta Z_{\text{ev ad}} = \frac{W_{\text{LWC}0}}{\beta_{\text{ad}}}. \quad (7)$$

Here

$$\beta_{\text{ad}} = \left(\frac{dW_{\text{LWC}}}{dz} \right)_{\text{ad}} \cong g \frac{\frac{LR_m}{C_p R_v T} - 1}{\frac{R_v T P}{E_s} + \frac{L^2 R_m}{C_p R_v T}}$$

is the adiabatic vertical gradient of liquid-water mixing ratio, P is the pressure of moist air, E_s is the saturation water vapour pressure at temperature T , L is the latent heat of

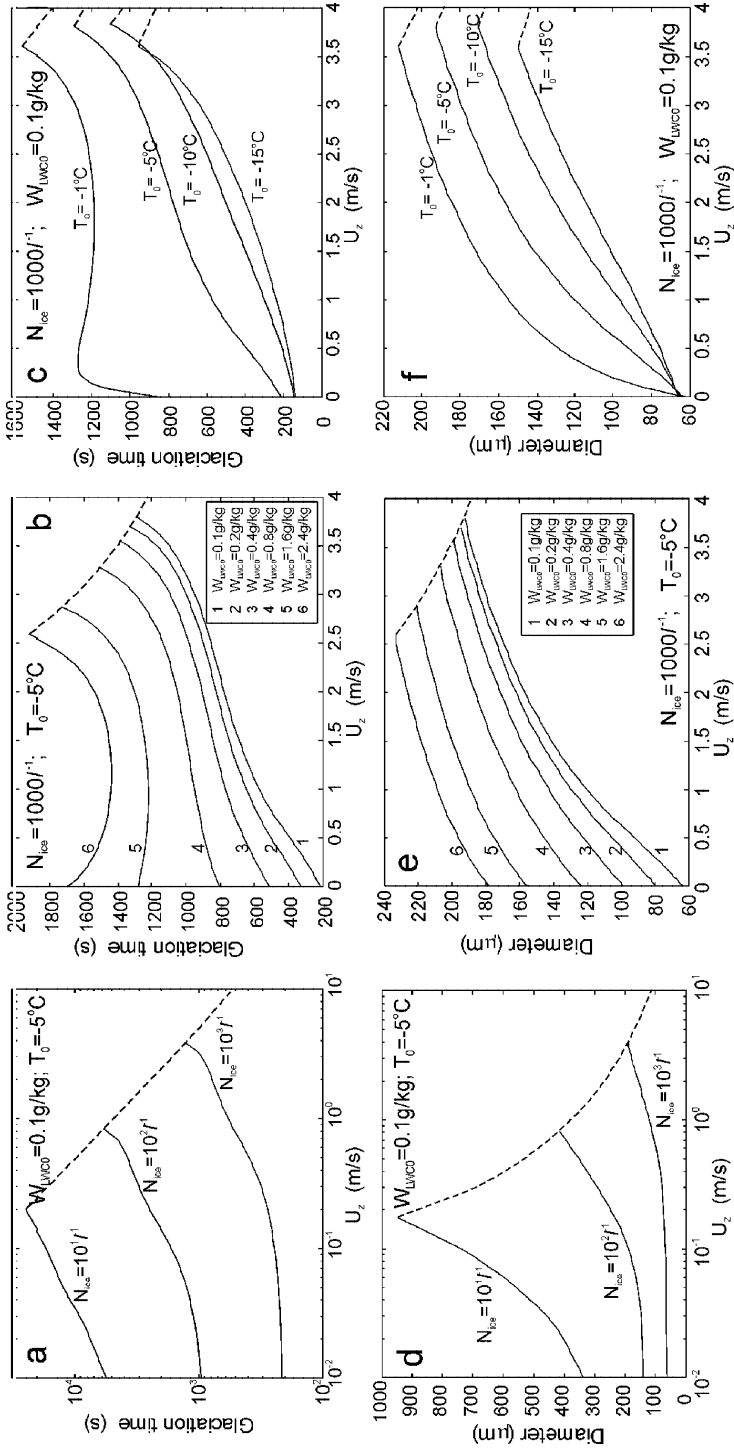


Figure 4. Glaciation time versus updraught velocity U_z for (a) different ice concentrations, (b) initial liquid-water content (W_{LWCO}), and (c) initial temperatures T_0 . Panels (d), (e) and (f) show sizes of ice spheres at the moment of glaciation versus U_z for different (d) ice concentrations, (e) W_{LWCO} , and (f) initial temperatures. Dashed lines indicate the spontaneous glaciation time when the parcel reaches $T = -40^\circ\text{C}$.

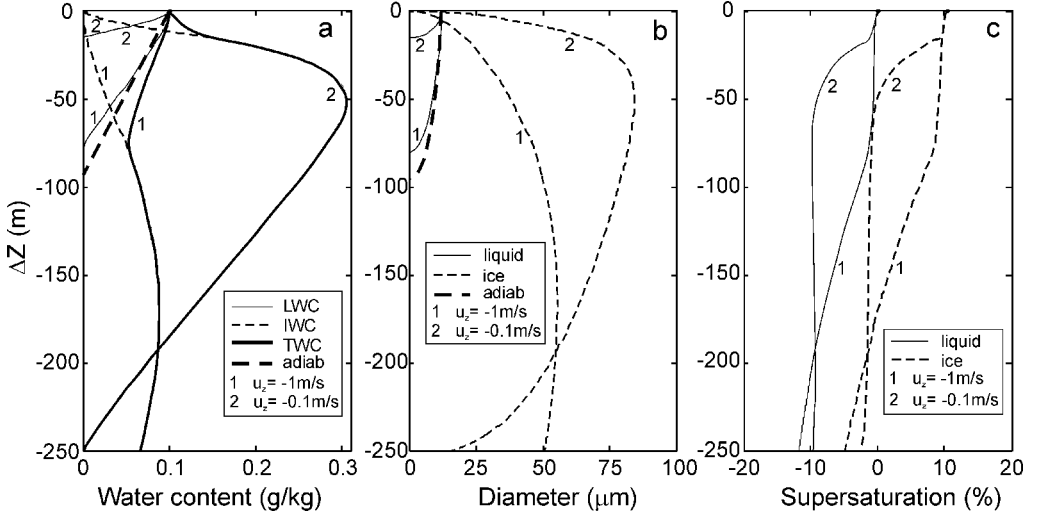


Figure 5. Modelling of phase transformation in a uniformly descending parcel for two different vertical velocities (1) $U_z = -1 \text{ m s}^{-1}$ and (2) $U_z = -0.1 \text{ m s}^{-1}$. Variation of (a) ice-water content (IWC), liquid-water content (LWC) and total water content (TWC); (b) liquid droplets and ice particle diameters; and (c) supersaturation over ice and liquid water. $N_i = 1000 \text{ l}^{-1}$, $T_0 = -10 \text{ }^\circ\text{C}$ and $H_0 = 1000 \text{ m}$ (see text). The thick dashed line refers to (a) adiabatic liquid-water content and (b) adiabatic droplet size.

condensation, C_p is the specific heat of moist air at constant pressure, R_m is the specific gas constant of moist air, and g is acceleration due to gravity. For a vertical displacement within a few hundreds of metres, to a good approximation, it can be assumed that $\beta_{\text{ad}} = \text{const}$ and the LWC changes linearly. If the parcel is moving down with a velocity U_z , then it will reach the level of droplet evaporation during the time

$$\tau_{\text{ev ad}} = \frac{W_{\text{LWC}0}}{U_z \beta_{\text{ad}}}. \quad (8)$$

In the presence of ice particles, the liquid droplets would evaporate faster, since ice particles act as an additional sink to the water vapour. Therefore, the droplet evaporation time will be smaller than that of Eq. (8), and $\tau_{\text{ev ad}}$ can be considered as an upper limit for the glaciation time τ_{gl} .

In Eqs. (7) and (8) it was assumed that the droplets evaporate instantly keeping the supersaturation equal to zero all the time. However, in a parcel moving down, condensation inertia, caused by a finite rate of evaporation, will cause the droplets to go a large distance as compared with $\Delta Z_{\text{ev ad}}$ before evaporation (Korolev and Mazin 1993). Thus, the actual evaporating time τ_{ev} is larger as compared with that calculated from Eq. (8), i.e. $\tau_{\text{ev}} > \tau_{\text{ev ad}}$. In this regard, instead of adiabatic $\tau_{\text{ev ad}}$, the glaciation time should be compared with the actual evaporation time of liquid droplets τ_{ev} . Figure 5 shows changes of LWC, IWC and TWC (Fig. 5(a)), diameters of droplet and ice particles (Fig. 5(b)), and supersaturation over ice and water (Fig. 5(c)) in a descending parcel having different velocities. As seen from Figs. 5(a) and (b), the smaller the downdraught velocity, the shorter the distance the parcel would pass before glaciation. It is interesting to note that in a slowly moving parcel ($U_z = -0.1 \text{ m s}^{-1}$) TWC reaches a maximum and then it starts to decrease (curve 2 in Fig. 5(a)), whereas in a fast descending parcel ($U_z = -1 \text{ m s}^{-1}$) TWC decreases first to a minimum and then starts increasing and decreasing again (curve 1 in Fig. 5(a)). Before evaporation of droplets, the supersaturation is close to saturation over water (full curves 1 and 2 in Fig. 5(c)). After droplet evaporation, the

supersaturation over ice decreases to approximately a zero value before ice sublimation at a low velocity $U_z = -0.1 \text{ m s}^{-1}$ (dashed curve 2 in Fig. 5(c)). Subzero supersaturation over ice is maintained by evaporating ice particles. At a higher downdraught velocity ($U_z = -1 \text{ m s}^{-1}$), the rate of change of supersaturation is so high that sublimating ice cannot maintain the supersaturation close to zero (dashed curve 1 in Fig. 5(c)). A comparison of the ice particle size changes (dashed curves 1 and 2 in Fig. 5(b)) also indicates that at a higher velocity ($U_z = -1 \text{ m s}^{-1}$) ice particles do not reach equilibrium and their size changes slower as compared with that at a lower velocity ($U_z = -0.1 \text{ m s}^{-1}$).

Figure 6 shows the dependence of (a) τ_{gl} and (b) D_{gl} versus U_z for different N_i . As seen from Fig. 6(a), τ_{gl} decreases with an increase of downdraught velocity. The thick dashed line indicates the adiabatic value of $\tau_{\text{ev ad}}$ calculated from Eq. (8). The grey line shows the actual evaporating time τ_{ev} of liquid droplets with no ice calculated from a numerical model (see an appendix). For smaller downdraught velocities, when the condensational inertia can be neglected, $\tau_{\text{ev ad}} > \tau_{\text{gl}}$ due to the effect of ice particles, which, in addition to the adiabatic heating, accelerate the evaporation of droplets. When the downdraught velocity increases, starting from a certain value, the effects of the condensation inertia become significant, resulting in the inequality $\tau_{\text{ev ad}} < \tau_{\text{gl}} < \tau_{\text{ev}}$. This effect can be seen in Fig. 6(a).

The size of ice particles D_{gl} in descending parcels decreases with an increase of the downdraught velocity (Fig. 6(b)). The values of D_{gl} for different N_i asymptotically approach each other when the downdraught velocity increases.

(d) Independence of the glaciation time on droplet size distribution

If the effects related to the condensation inertia of droplets are negligible, τ_{gl} does not depend on the shape of the droplet size distribution, but depends on its third moment, or liquid water content. Figure 7 demonstrates the independence of τ_{gl} on the shape of droplet spectra. The glaciation time was calculated for a vertically moving parcel having the same initial W_{LWC0} but different droplet concentration and, therefore, initial droplet radius. As seen from Fig. 7, τ_{gl} stays approximately the same for all the cases with $N > 50 \text{ cm}^{-3}$ and $W_{\text{LWC0}} = 0.1 \text{ g kg}^{-1}$. When the concentration of droplets becomes comparable with that of ice (curves $N = 1 \text{ cm}^{-3}$ and $N = 10 \text{ cm}^{-3}$ in Fig. 7), τ_{gl} starts to deviate noticeably from the cases when the concentration is high and the droplets are small. Typically the concentration of cloud droplets is two orders of magnitude higher as compared with the concentration of ice particles. Therefore, τ_{gl} may be considered independent of the shape of the droplet size distribution for the majority of clouds.

(e) Variation of ice water fraction in a uniformly vertically moving parcel

During glaciation, the ice water fraction $\mu_3(t) = \text{IWC}/\text{TWC}$ changes from 0, when the cloud is liquid, to 1 when the cloud is completely glaciated. Figure 8 shows the dependence of μ_3 versus normalized glaciation time, $\Delta\tau/\tau_{\text{gl}} = (\tau_{\text{gl}} - t)/\tau_{\text{gl}}$, for different vertical velocities, calculated for $W_{\text{LWC0}} = 0.1 \text{ g kg}^{-1}$, $T_0 = -15 \text{ }^\circ\text{C}$ and $H_0 = 1000 \text{ m}$. As seen from Fig. 8, μ_3 changes in a near linear manner with time when $U_z = 0$. However, $\Delta\tau/\tau_{\text{gl}}$ may be significantly different from the above when $U_z \neq 0$. Comparison of Fig. 8(a) and (b) indicates that $\mu_3(\Delta\tau/\tau_{\text{gl}})$ for the zero-velocity case increases with an increase of the absolute value of U_z and N_i . Besides U_z and N_i , the shape of the curves μ_3 versus $\Delta\tau/\tau_{\text{gl}}$ depends on initial LWC, temperature and pressure. The results shown in Fig. 8 clearly indicate that no steady state is possible for $0 < \mu_3 < 1$ when glaciation occurs solely due to the WBF mechanism.

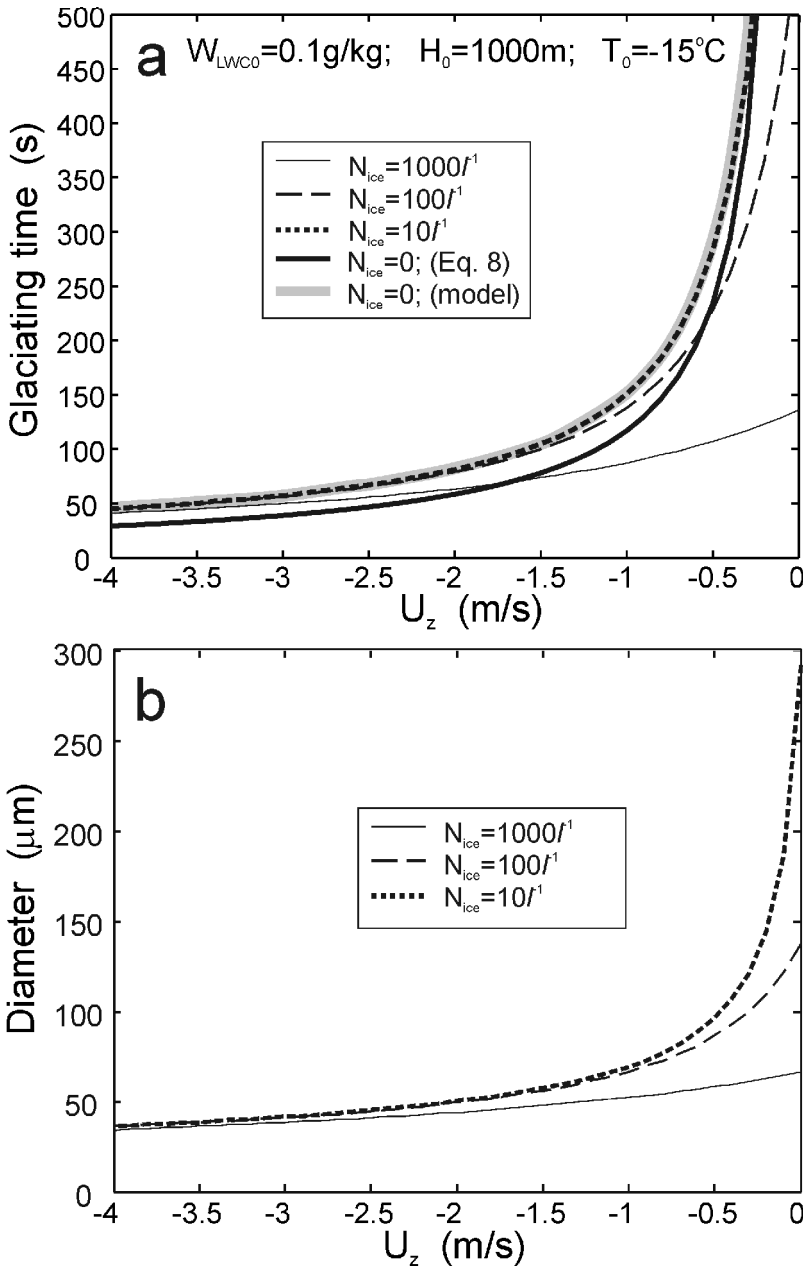


Figure 6. (a) Glaciation time and (b) ice sphere diameter at the moment of glaciation versus velocity of the descending parcel for various number concentrations of ice particles: $W_{LWC0} = 0.1 \text{ g kg}^{-1}$, $H_0 = 1000 \text{ m}$, $T_0 = -15^\circ \text{C}$ and $N_{\text{dropl}} = 100 \text{ cm}^{-3}$ (see text).

(f) *Oscillating U_z*

Cloud parcels in stable layers may perform random or periodic fluctuations related to turbulence, gravity waves, or Kelvin–Helmholtz instability. The effect of the vertical fluctuations on the formation of droplet size spectra in liquid clouds was discussed in detail by Korolev (1995). Such fluctuations may completely change the scenario

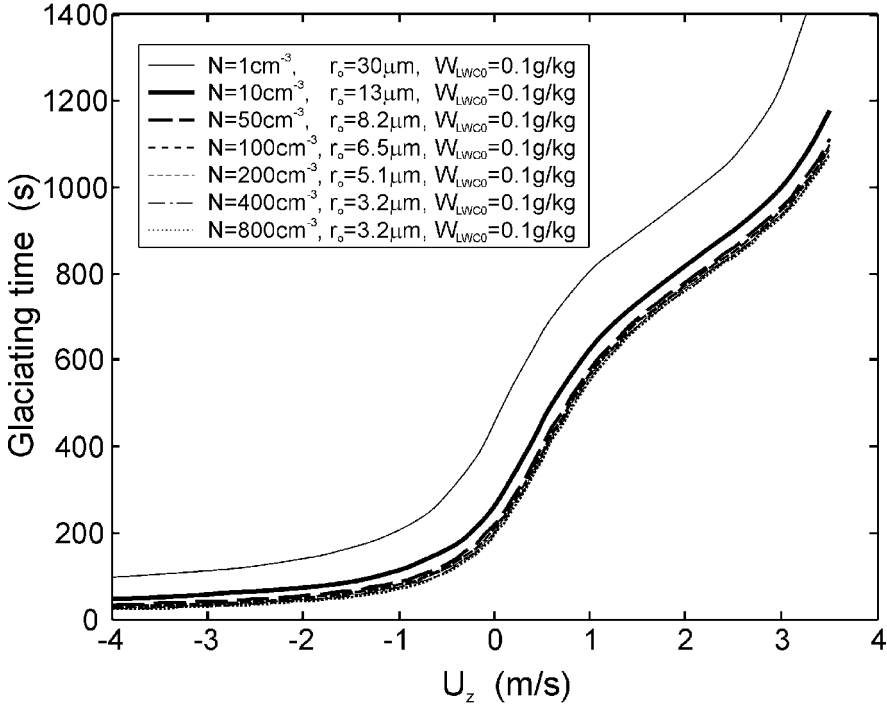


Figure 7. Glaciation time versus vertical velocity for adiabatic parcels having the same initial water content but different droplet concentration, N , and initial droplet radius r_0 . $W_{LWCO} = 0.1 \text{ g kg}^{-1}$, $N_i = 1000 \text{ l}^{-1}$, $T_0 = -10 \text{ }^\circ\text{C}$ and $H_0 = 1000 \text{ m}$ (see text).

of the phase transformation as compared with the uniform vertical motion as was discussed in sections 3(b) and (c). Figures 9, 10 and 11 show modelled changes of LWC, IWC, sizes of droplets and ice particles, and supersaturation over ice and liquid water in a periodically up and down moving cloud parcel. The radius of the vortex was assumed $R = 100 \text{ m}$, the tangential velocity $u_r = 0.5 \text{ m s}^{-1}$, initial $W_{LWCO} = 0.1 \text{ g kg}^{-1}$ and $T_0 = -5 \text{ }^\circ\text{C}$. The model was run for three different ice number concentrations $N_i = 10 \text{ l}^{-1}$ (Fig. 9), $N_i = 100 \text{ l}^{-1}$ (Fig. 10), and $N_i = 1000 \text{ l}^{-1}$ (Fig. 11). The stars on the time axis (Figs. 9(a), 10(a) and 11(a)) indicate the glaciation time for $U_z = 0$. In the case of vertical fluctuations for $N_i = 10 \text{ l}^{-1}$ (Fig. 9), the liquid droplets periodically evaporate in downdraughts and activate in updraughts keeping the cloud in mixed phase significantly longer as compared with τ_{gl} when $U_z = 0$. The amplitude of LWC fluctuations gradually decreases until, in approximately 4 hours, it reaches its constant value of about 0.025 g kg^{-1} . By this time, IWC and ice particle diameter, D_i , averaged over one cycle reach stationary values. For $N_i = 100 \text{ l}^{-1}$ (Fig. 10), the amplitude of LWC decreases more rapidly as compared with the previous case and then it stabilizes at 0.02 g kg^{-1} in approximately 1.5 hours. For the case of $N_i = 1000 \text{ l}^{-1}$ (Fig. 11) after the first cycle of evaporation, liquid droplets do not activate anymore. In all three cases, IWC after some time starts to oscillate around the same average value 0.35 g kg^{-1} , though the amplitude of the oscillations increases with the increase of N_i (compare Figs. 9(a), 10(a) and 11(a)). It is worth noting that, in all three cases, the amplitude of ice (S_i) and water (S_w) supersaturation and averaged IWC and D_i reach a steady state.

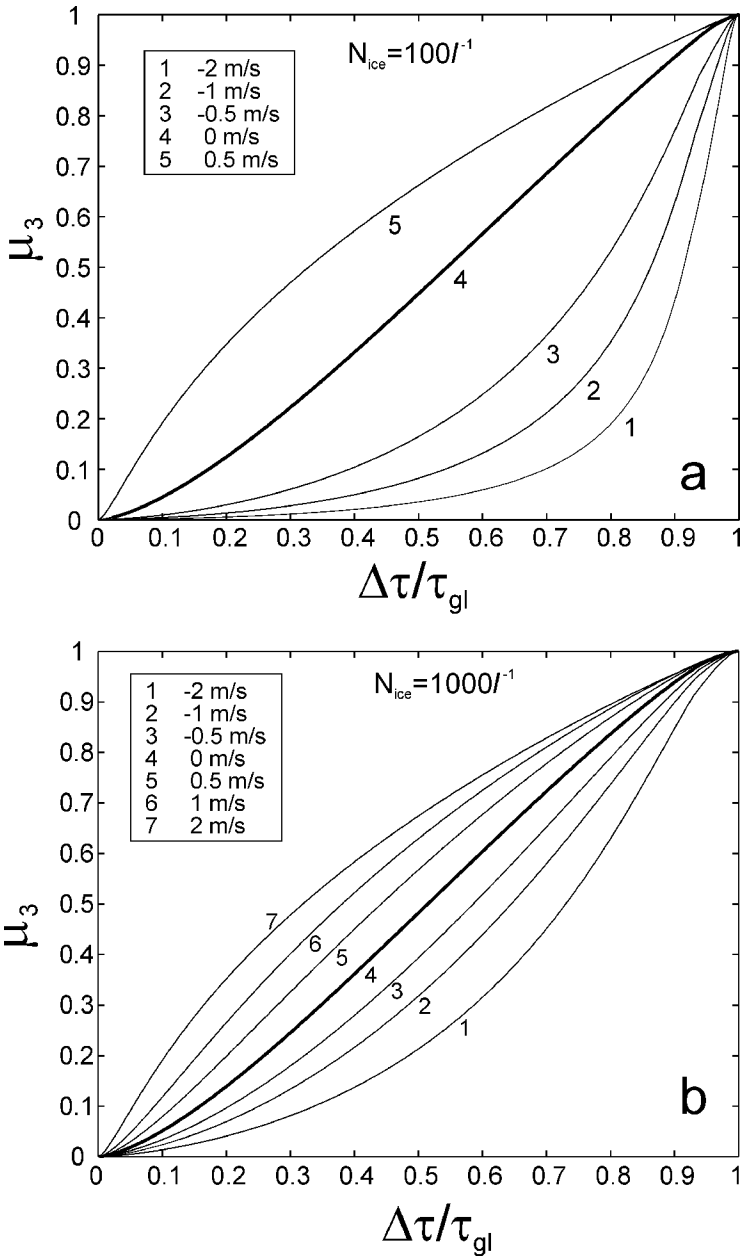


Figure 8. Dependence of the phase composition coefficient μ_3 versus normalized glaciation time for different vertical velocities at $H_0 = 1000$ m, and $T_0 = -10$ °C (see text) for different number concentrations of ice particles: (a) $N_i = 100 \text{ l}^{-1}$, and (b) $N_i = 1000 \text{ l}^{-1}$.

The amplitude of oscillations of IWC and D_i increase and that of S_i decreases with an increase of N_i . Such dependence is related to the rate of water vapour absorption or release by an ensemble of cloud particles. The characteristic time of changes in water vapour due to condensation processes, or the time of phase relaxation, τ_{ph} , is proportional to $1/N_i \bar{D}_i$ (Mazin 1968). As τ_{ph} gets lower, cloud particles absorb or release water vapour faster. Therefore, a cloud parcel having a larger τ_{ph} would have

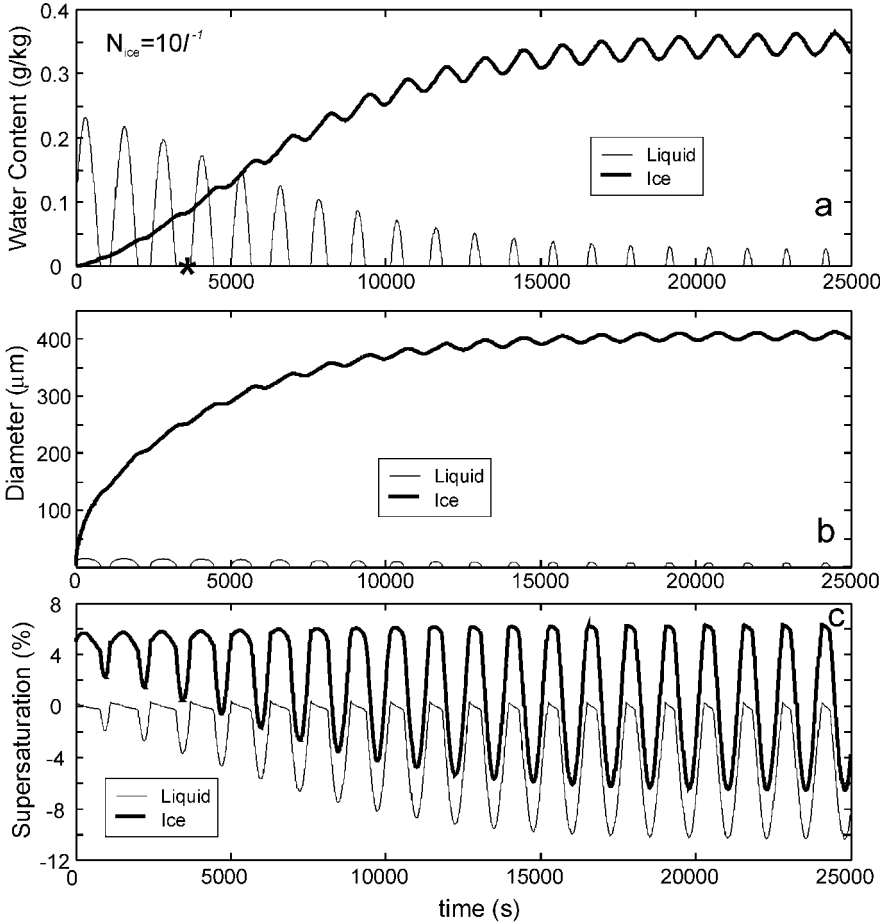


Figure 9. Modelling of phase transformation in a periodically moving up and down parcel. The radius of the vortex $R = 100$ m, the tangential velocity $u_r = 0.5$ m s $^{-1}$, $N_i = 10$ l $^{-1}$, $W_{LWC0} = 0.1$ g kg $^{-1}$, $T_0 = -5$ °C, and $H_0 = 1000$ m (see text). Changes of (a) ice-water content and liquid-water content (a star on the time axis denotes glaciation time for zero vertical velocity), (b) ice particle diameter, and (c) supersaturation over ice and water.

larger condensation inertia and it will be less sensitive to the changes of supersaturation caused by external factors, as compared with a parcel having smaller τ_{ph} . After the IWC reaches a steady state, the average diameter of ice particles for the case $N_i = 10$ l $^{-1}$ will be about $D_i = 400$ μ m (Fig. 9). For the case $N_i = 1000$ l $^{-1}$ shown in Fig. 11, the average diameter will be about $D_i = 80$ μ m. Therefore, τ_{ph} is 20 times higher for the case shown in Fig. 9 as compared with that in Fig. 11. This explains the smaller amplitudes of IWC and D_i and larger amplitudes for S_i in Fig. 11 as compared with that of Fig. 9. Since the ice particles at lower concentrations have less capability to adapt to changes of supersaturation, the supersaturation at a certain point may exceed saturation over water and result in activation of liquid droplets (Figs. 9 and 10). Numerical modelling showed that the activation of liquid water in a vertically oscillating parcel in the presence of ice particles depends on N_i , W_{LWC0} , c , T_0 , H_0 , u_r , and the radius of oscillations R . A decrease of the ice particle shape factor c would result in activation of liquid droplets at higher N_i .

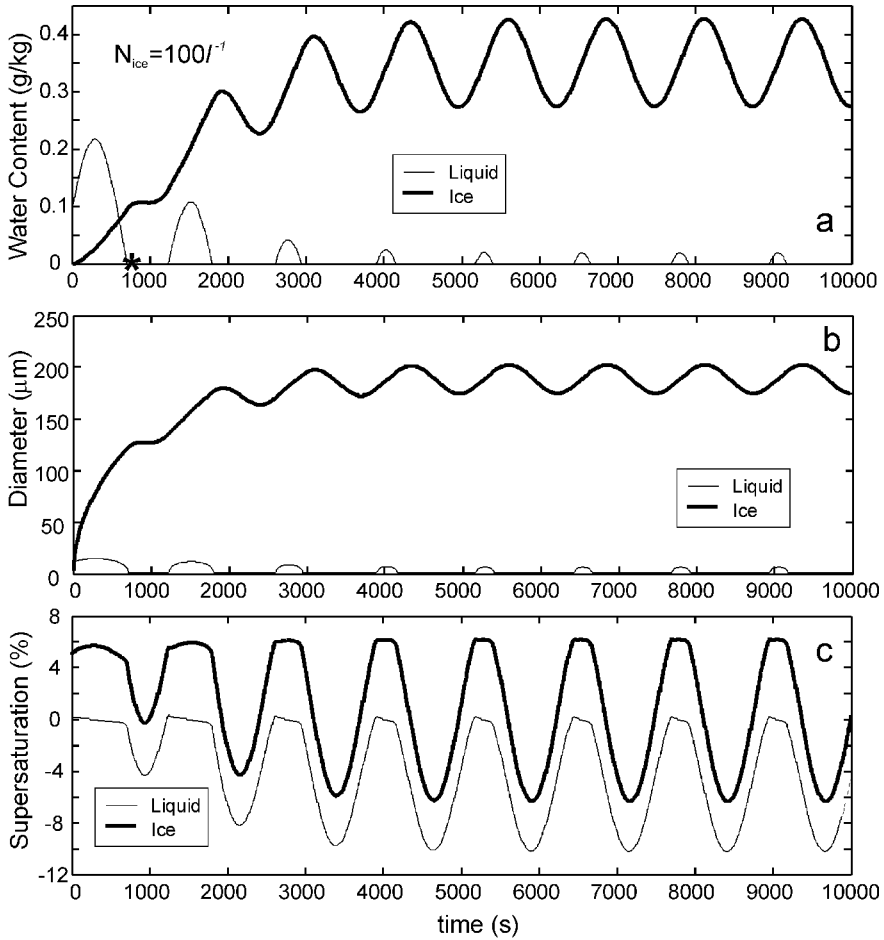


Figure 10. Same as in Fig. 9 but for $N_i = 100 \text{ l}^{-1}$.

3. DISCUSSION

(a) Limitations of the WBF mechanism in cloud glaciation

The glaciation of a mixed-phase cloud as considered in section 2 is rather simplified and it does not take into account such important phenomena as the ventilation effect (Keller and Hallett 1982; Alena *et al.* 1990), riming (e.g. Takahashi and Fukuta 1988), the effect of ice particle shape on the growth rate (e.g. Mason 1994), terminal fall velocity (e.g. Locatelli and Hobbs 1974) and ice nucleation, entrainment and mixing. A detailed review of the above subjects can be found by Pruppacher and Klett (1997). The ventilation effect and riming would result in an enhanced growth of the ice particles and a reduction of the droplet number concentration, which would decrease τ_{gl} . The particle habit is related to the temperature and supersaturation (e.g. Nakaya 1954; Kobayashi 1957; Hallett and Mason 1958; Rottner and Vali 1974; Fukuta and Takahashi 1999). Since in our case the supersaturation is close to that over water, the growth rate is expected to be dependent on temperature only. The rate of mass growth is rather close to Maxwellian (Eq. (1)) (e.g. Fukuta and Takahashi 1999). That supports the use of Eq. (5) as an estimate of τ_{gl} . Ice nucleation and ice multiplication (Hallett and Mossop 1974)

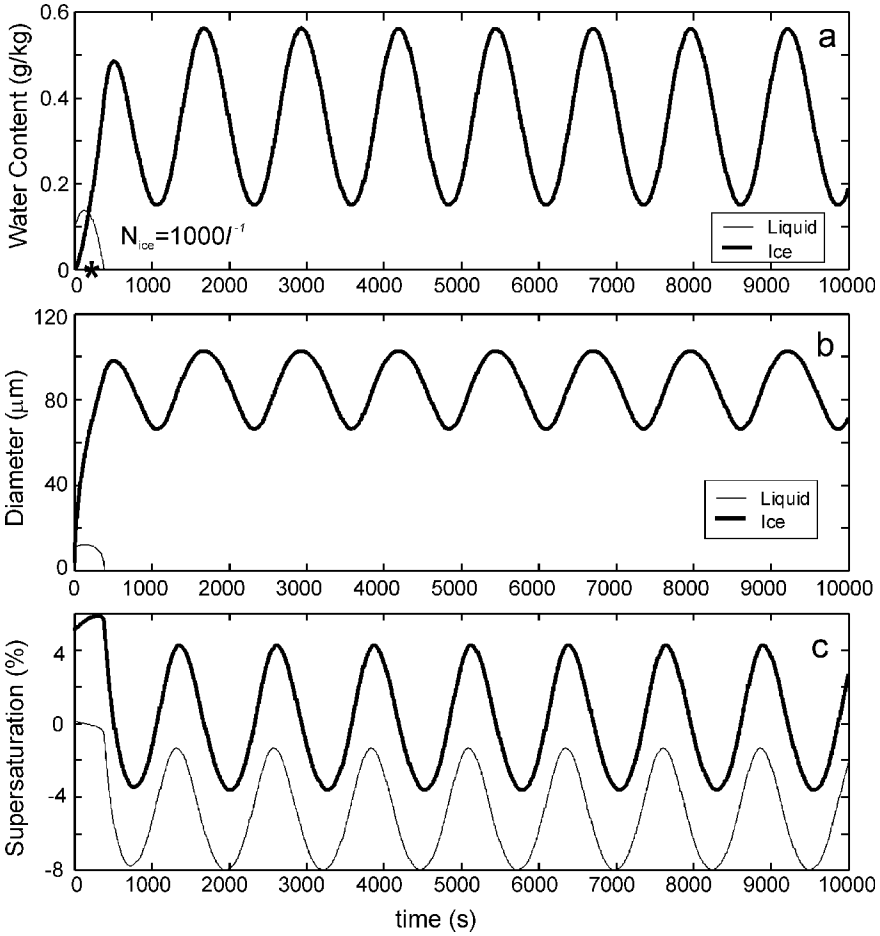


Figure 11. Same as in Fig. 9. but for $N_i = 1000 \text{ l}^{-1}$.

may affect ice particle concentration that would reduce τ_{gl} . The terminal fall velocity would reduce the residence time of ice particles in the cloud volume that would lead to an increase of τ_{gl} . Pinto (1998) and Harrington *et al.* (1999) suggested that ice particles falling out of a cloud might significantly increase τ_{gl} .

The above mechanisms may both increase and decrease τ_{gl} . In a complex way, the resulting effect depends on a number of different parameters, e.g. size distributions of ice particles and liquid droplets, LWC, T , H , etc, so there is no unambiguous answer on how the actual glaciation time would relate to that derived for the WBF mechanism only. Therefore, τ_{gl} derived in this study should be considered only as an estimate.

Changing some of the constants used in the growth rate of ice particles may affect τ_{gl} . The ‘capacitance’ c used in the ice crystal growth equation was set to $c = 1$ to represent spherical particles. Depending on the particle habit, c may vary in the range $0 < c < 1$. Reducing c would increase τ_{gl} linearly with c^{-1} for the case $U_z = 0$ (Eq. (6)). If $U_z \neq 0$ τ_{gl} would change nonlinearly with c^{-1} . Ice particle density was nominally set to $\rho_i = 900 \text{ kg m}^{-3}$. Reducing ρ_i also increases τ_{gl} . The coefficients of thermal accommodation, ice deposition and condensation were set to 1 in Eqs. (1), (A.4) and (A.5). Changing these coefficients has only a small effect.

Due to the idealized assumptions used in this study, the model is expected at certain points to break down with unrealistic results. For example, because of large ice particle fallout, complete cloud glaciation may never occur. The terminal fall velocity of an ice particle is governed mainly by its shape and dimensions. Figures 4(d), (e) and (f) and 6(b) show D_{gl} at the moment of glaciation τ_{gl} . As seen from Figs. 4(d) to (f) the sizes of ice spheres at $N_i = 1000 \text{ l}^{-1}$ and $W_{LWC0} = 0.1 \text{ g kg}^{-1}$ vary in the range $60 \mu\text{m} < D_{gl} < 220 \mu\text{m}$. The terminal fall velocity U_{fall} of such spheres varies as $0.1 \text{ m s}^{-1} < U_{fall} < 0.7 \text{ m s}^{-1}$, respectively. Since a sphere gives the smallest size for the same mass, it is expected that real ice particles would have larger sizes, and their terminal fall velocity will be lower. On the other hand, the fall velocity of 1 mm unrimed aggregates of plates, bullets and columns does not exceed 0.7 m s^{-1} (Locatelli and Hobbs 1974). The initial size of the ice particle was set to $D_{i0} = 1 \mu\text{m}$. Thus during glaciation the size of ice particles changed in the range $D_{i0} < D_i < D_{gl}$. The average velocity of growing ice particles can be roughly estimated as 50% of the fall speed at the moment of glaciation. In order for glaciation to occur, the ice particles should stay in the parcel all the time. For the case $N_i = 1000 \text{ l}^{-1}$ and $W_{LWC0} = 0.1 \text{ g kg}^{-3}$ the glaciation time varies from 200 s to 1200 s (Fig. 4(b)). Therefore, the size of the parcels can be estimated as $\Delta x \sim \tau_{gl} U_{fall}/2$, which yields $10 \text{ m} < \Delta x < 420 \text{ m}$. The size of such cloud parcels and their lifetime, determined by τ_{gl} , look realistic for both stratiform and convective clouds. However, concentrations of ice particles lower than 100 l^{-1} would result in larger τ_{gl} , D_{gl} (Fig. 4) and, therefore, larger U_{fall} , and unrealistically large cloud parcel sizes $\Delta x > 10^3 \text{ m}$. As a result, at such concentrations, the modelling of the glaciation due to the WBF mechanism may break down.

In order for cloud (or cloud parcel) glaciation to occur due to the WBF mechanism, the residence time of cloud particles should be no less than the glaciating time. If this condition is not satisfied then the glaciated clouds at $T > -40^\circ\text{C}$ would never be observed. The glaciation of a cloud at $N_i < 10 \text{ l}^{-1}$ would require about a few hours (Figs. 1 and 4(a)). This time looks unrealistically high since ice particles would grow to large sizes and therefore they would have a higher terminal fall velocity (Figs. 4(a) and (d)) which would reduce their residence time inside the cloud.

Recent studies of the phase composition of stratiform clouds by Korolev *et al.* (2003) suggest that glaciated clouds are observed rather frequently at $-35^\circ\text{C} < T < 0^\circ\text{C}$. The mean volume diameter of particles in glaciated clouds was found to be about $20 \mu\text{m}$ to $40 \mu\text{m}$ (Korolev *et al.* 2003) and their concentration about $2\text{--}5 \text{ cm}^{-3}$ (Gultepe *et al.* 2001; Korolev *et al.* 2003). The results of modelling and experimental observations of microstructure of mixed and ice clouds (Korolev *et al.* 2003) suggest that the WBF mechanism in some cases may be solely responsible for glaciation of natural clouds.

(b) *The effect of cloud dynamics on mixed-phase composition*

Modelling of mixed-phase transformation in Figs. 9–11 indicates that after some time IWC and LWC may start oscillating around some average values, which stay constant with time. This yields an important conclusion that phase transformation in a fluctuating up-and-down parcel is significantly different as compared with a uniformly moving parcel. Early works by Bergeron (1935) and Findeizen (1938) suggested that at $U_z = 0$ the mixture of ice and liquid droplets is fundamentally unstable. As was shown above, the same conclusion is valid for a vertically moving parcel having a constant velocity. However, for an oscillating U_z under certain conditions, it is possible to achieve a periodic evaporation and activation of liquid water keeping the system, on average, in a mixed-phase condition during an infinitesimally long time. In this case we may speculate that a steady-state condition for a mixed phase may be reached *on*

average for a vertically fluctuating parcel. The steady-state condition is not achievable in principle for a uniformly vertically moving parcel. This conclusion is very important for understanding phase transformation of clouds and the characteristic time of glaciation. Based on this numerical modelling, it is hypothesized that turbulent clouds, or clouds with regular motions generated by gravity waves of Kelvin–Helmholtz instability, would stay longer in a mixed condition as compared to ‘quiet’ ones. Vertical oscillations may also provide an additional explanation for the long-lived mixed-phase stratiform sheets discussed by Rauber and Tokay (1991), Harrington *et al.* (1999), and Pinto (1998).

4. CONCLUSIONS

In this study the following results were obtained:

(a) For the case $U_z = 0$, the glaciation time through the Wegener–Bergeron–Findeisen mechanism is proportional to $(W_{\text{LWC0}}/N_i)^{2/3}$, and to a first approximation does not depend on the shape of the droplet size distribution. The characteristic time of glaciation is about 10^2 s for $W_{\text{LWC0}} \sim 0.1$ g kg⁻¹ and $N_i \sim 10^3$ l⁻¹ for the assumption that ice particles are spheres ($c = 1$). If $N_i < 10^2$ l⁻¹ then $\tau_{\text{gl}} > 10^3$ s, i.e. the cloud may stay in a mixed condition for hours. For non-spherical particles τ_{gl} should be scaled proportional to c^{-1} .

(b) The glaciation time in updraughts is a complex function of initial T_0 , P_0 , W_{LWC0} , N_i , c and U_z . The glaciation time may both increase and decrease in updraughts with an increase of U_z . The glaciation time in descending parcels increases with an increase of downdraught velocity. Numerical modelling shows that glaciation in convective clouds having $N_i < 1000$ l⁻¹ and $U_z > 4$ m s⁻¹ would never occur through the WBF mechanism before it reaches a level with $T = -40$ °C. After this, glaciation occurs through spontaneous freezing.

(c) No steady state is possible for IWC/TWC in a uniformly vertically moving mixed-phase parcel.

(d) The vertical oscillation of a cloud parcel may result in a periodic evaporation and activation of liquid droplets in the presence of ice particles. After a certain time, the *average* IWC and LWC reaches a steady state. This phenomenon may explain the existence of long-lived mixed-phase stratiform layers.

ACKNOWLEDGEMENTS

Alexei Korolev performed this work under contract KM175-012030/001/TOR to the Meteorological Service of Canada. The Panel of Energy Research and Development, and the National Search and Rescue Secretariat provided funding for this work. The authors appreciate comments of the anonymous reviewers, which helped to improve the paper.

APPENDIX

The process of cloud phase transformation in an adiabatic parcel can be described by a system of the following equations. The glaciation time was calculated using the following equations:

the pressure variation equation,

$$\frac{dP}{dt} = -\frac{gPU_z}{R_m T}; \quad (\text{A.1})$$

the energy conservation equation,

$$\frac{dT}{dt} = -\frac{gU_z}{C_p} + \frac{L_1}{(1+q_v)C_p} \frac{dq_l}{dt} + \frac{L_i}{(1+q_v)C_p} \frac{dq_i}{dt}; \quad (\text{A.2})$$

the water mass conservation equation,

$$\frac{dq_v}{dt} + \frac{dq_l}{dt} + \frac{dq_i}{dt} = 0; \quad (\text{A.3})$$

the liquid droplets mass,

$$\frac{dq_l}{dt} = 4\pi A_1 N_1 r_1 S_1; \quad (\text{A.4})$$

and the ice particles mass,

$$\frac{dq_i}{dt} = 4\pi c A_i N_i r_i S_i. \quad (\text{A.5})$$

Equations (A.1)–(A.5) employed the following symbols: P , pressure of moist air; T , temperature; q_v , q_l and q_i , water vapour, condensed liquid and ice mass per unit mass of dry air, respectively; U_z , vertical velocity; r , cloud particle radius; g , acceleration of gravity; L_1 , L_i , latent heat for liquid and ice, respectively; N_l , N_i , total number of droplets and ice particles in a closed volume of air per unit mass, respectively; R_m , R_v , specific gas constant of moist air and water vapour, respectively; C_p , specific heat capacity of moist air at constant pressure; $S = E/E_s - 1$, supersaturation; E , vapour pressure far from a cloud particle; $E_s(T)$, saturation vapour pressure above a flat surface of water or ice; c is a constant ‘capacitance’ representing the ice crystal habit ($c = 1$ for spheres);

$$A_l = \left(\frac{L_1^2}{kR_v T^2} + \frac{R_v T}{E_{sl}(T)D} \right)^{-1}, \quad A_i = \left(\frac{L_i^2}{kR_v T^2} + \frac{R_v T}{E_{si}(T)D} \right)^{-1}$$

coefficients in liquid and ice growth Eq. (A.4) and (A.5), respectively; D , the coefficient of water vapour diffusion in air; k , the coefficient of air heat conductivity. For $k(T)$ and $L(T)$ the dependence on temperature was taken into account. For $D(T, P)$ both temperature and pressure were considered. Subscript l and i refer to liquid and ice, respectively. The ice particles in the above model were assumed spheres, having initial size $r_i(t_0) = 1 \mu\text{m}$. If not specified in the text or figure captions, the droplet number concentration was $N_l = 100 \text{ cm}^{-3}$.

REFERENCES

- | | | |
|---|------|--|
| Alena, T., Hallett, J. and Saunders, C. P. R. | 1990 | On the facet–skeletal transition of snow crystals: Experiments in high and low gravity. <i>J. Cryst. Growth</i> , 104 , 539–555 |
| Bergeron, T. | 1935 | ‘On the physics of clouds and precipitation’. Pp. 156–178 in <i>Procès Verbaux de l’Association de Météorologie, International Union of Geodesy and Geophysics</i> , Paris, France |
| Bower, K. N., Moss, S. M., Johnson, D. W., Choulaton, T. W., Latham, J., Brown, P. R., Blyth, A. and Cardwell, J. | 1996 | A parametrization of ice water content observed in frontal and convective clouds. <i>Q. J. R. Meteorol. Soc.</i> , 122 , 1815–1844 |
| Cotton, W. R. and Anthes, R. A. | 1989 | <i>Storm and cloud dynamics</i> . International Geophysics Series, Vol. 44. Academic Press, New York, USA |
| Findeisen, W. | 1938 | Kolloid-meteorologische Vorgänge bei Neiderschlags-bildung. <i>Meteorologische Zeitschrift</i> , 55 , 121–133 |

- Fletcher, N. H. 1962 *Physics of rain clouds*. Cambridge University Press, Cambridge, UK
- Fukuta, N. and Takahashi, T. 1999 The growth of atmospheric ice crystals: A summary of findings in vertical supercooled cloud tunnel studies. *J. Atmos. Sci.*, **56**, 1963–1979
- Fukuta, N. and Walter, L. A. 1970 Kinetics of hydrometeor growth from a vapour spherical model. *J. Atmos. Sci.*, **27**, 1160–1172
- Gultepe, I., Isaac, G. A. and Cober, S. G. 2001 Ice crystal number concentration versus temperature. *Int. J. Climatol.*, **21**, 1281–1302
- Hall, W. D. 1980 A detailed microphysical model within a two-dimensional dynamic framework: Model description and preliminary results. *J. Atmos. Sci.*, **37**, 2486–2507
- Hallett, J. and Mason, B. J. 1958 The influence of temperature and supersaturation on the habit of ice crystals grown from the vapour. *Proc. R. Soc. London*, **A247**, 440–453
- Hallett, J. and Mossop, S. C. 1974 Production of secondary ice particles during the riming process. *Nature*, **249**, 26–28
- Harrington, J. Y., Reisin, T., Cotton, W. R. and Kreidenweis, S. M. 1999 Cloud resolving simulation of Arctic stratus. Part II: Transition-season clouds. *Atmos. Res.*, **51**, 45–75
- Houze, R. A. 1992 *Cloud dynamics*. International Geophysics Series, Vol. 53. Academic Press, New York, USA
- Jiang, H., Cotton, W. R., Pinto, J. O., Curry, J. A. and Weissbluth, M. J. 2000 Cloud resolving simulations of mixed-phase Arctic stratus observed during BASE: sensitivity to concentration of ice crystals and large-scale heat and moisture advection. *J. Atmos. Sci.*, **57**, 2105–2117
- Juisto, J. E. 1971 Crystal development and glaciation of a supercooled cloud. *J. Res. Atmos.*, **5**, 69–85
- Keller, V. W. and Hallett, J. 1982 Influence of air velocity on the habit of ice crystal growth from the vapour. *J. Cryst. Growth*, **60**, 91–106
- Kobayashi, T. 1957 Experimental researches on the snow crystal habit and growth by means of a diffusion cloud chamber. *J. Meteorol. Soc. Jpn. 75th Anniv. Vol.*, 38–44
- Korolev, A. V. 1995 The influence of supersaturation fluctuation on droplet size spectra formation. *J. Atmos. Sci.*, **52**, 3620–3634
- Korolev, A. V. and Mazin, I. P. 1993 Zones of increased and decreased droplet number concentration in stratiform clouds. *J. Appl. Meteorol.*, **32**, 760–773
- Korolev, A. V., Isaac, G. A., Cober, S. G., Strapp, J. W. and Hallett, J. 2003 Microphysical characterization of mixed-phase clouds. *Q. J. R. Meteorol. Soc.*, **129**, 39–65
- Locatelli, R. M. and Hobbs, P. V. 1974 Fallspeed and masses of solid precipitating particles. *J. Geophys. Res.*, **79**, 2185–2197
- Lohmann, U. and Roeckner, E. 1996 Design and performance of a new cloud microphysics scheme developed for the ECHAM general circulation model. *Cloud Dynamics*, **12**, 557–572
- McClatchey, R. A., Fenn, R. W., Selby, J. E. A., Volz, F. E. and Garing, J. S. 1972 ‘Optical properties of the atmosphere’. 3rd ed., Environmental Research Paper, No 411, AFCRL-72-0497, [NTIS N7318412], Bedford, Massachusetts, USA
- Mason, B. J. 1994 The shapes of snow crystals—Fitness for purpose? *Q. J. R. Meteorol. Soc.*, **120**, 849–860
- Mazin, I. P. 1968 ‘The stochastic condensation and its effect on the formation of cloud droplet size distribution’. Pp. 67–71 in Proceedings of an international conference on cloud physics, August 26–30, Toronto, Canada
- 1983 Phase changes in clouds. *Soviet Meteorology and Hydrology*, **7**, 26–34
- Mazin, I. P., Korolev, A. V. and Isaac, G. A. 2000 ‘Phase transition in clouds’. Pp. 657–660 in Proceedings of the 13th international conference on clouds and precipitation, Reno, 14–18 August 2000. Desert Research Institute, Nevada, USA
- Meyers, M. P., DeMott, P. J. and Cotton, W. R. 1992 New primary ice-nucleation parameterizations in an explicit cloud model. *J. Appl. Meteorol.*, **31**, 708–721
- Nakaya, U. 1954 *Snow crystals, natural and artificial*. Harvard University Press, Cambridge, MA, USA
- Pinto, J. O. 1998 Autumnal mixed-phase cloudy boundary layers in the Arctic. *J. Atmos. Sci.*, **55**, 2016–2038

- Pruppacher, H. R. and Klett, J. D. 1997 *Microphysics of clouds and precipitation*. Kluwer Academic Publisher, London
- Rauber, R. M. and Tokay, A. 1991 An explanation for the existence of supercooled water at the top of cold clouds. *J. Atmos. Sci.*, **55**, 2016–2038
- Reisin, T., Levin, Z. and Tzivion, S. 1996 Rain production in convective clouds as simulated in an axisymmetric model with detailed microphysics. Part I: Description of the model. *J. Atmos. Sci.*, **53**, 497–520
- Rotstajn, L. D., Ryan, B. F. and Katzfey, J. J. 2000 A scheme for calculation of the liquid fraction in mixed-phase stratiform clouds in large-scale models. *Mon. Weather Rev.*, **128**, 1070–1088
- Rottner, D. and Vali, G. 1974 Snow crystal habit at small excesses of vapour density over ice saturation. *J. Atmos. Sci.*, **31**, 560–569
- Ryan, B. F., Wishart, E. R. and Shaw, D. E. 1976 The growth rates and densities of ice crystals between -3°C and -21°C . *J. Atmos. Sci.*, **33**, 53–70
- Schols, J. L., Weinman, J. A., Alexander, G. D., Stewart, R. E., Angus, L. J. and Lee, A. C. L. 1999 Microwave properties of frozen precipitation around a North Atlantic cyclone. *J. Appl. Meteorol.*, **38**, 29–43
- Scott, B. C. and Hobbs, P. V. 1977 A theoretical study of the evolution of mixed-phase cumulus clouds. *J. Atmos. Sci.*, **34**, 812–826
- Takahashi, T. and Fukuta, N. 1988 Supercooled cloud tunnel studies in the growth of snow crystals between -4°C and -20°C . *J. Meteorol. Soc. Jpn*, **66**, 841–855
- Tremblay, A., Glazer, A. and Benoit, W. Yu. R. 1996 A mixed-phase cloud scheme based on a single prognostic equation. *Tellus*, **48**, 483–500
- Wegener, A. 1911 *Thermodynamik der Atmosphäre*. Leipzig, Poland
- Zawadzki, I., Szyrmer, W. and Laroche, S. 2000 Diagnostic of supercooled clouds from single-Doppler observations in regions of radar-detectable snow. *J. Appl. Meteorol.*, **39**, 1041–1058